The Journal of Immunology

Acute Serum Amyloid A Induces Migration, Angiogenesis, and Inflammation in Synovial Cells In Vitro and in a Human Rheumatoid Arthritis/SCID Mouse Chimera Model

Mary Connolly, Alessandra Marrelli, Mark Blades, Jennifer McCormick, Paola Maderna, Catherine Godson, Ronan Mullan, Oliver FitzGerald, Barry Bresnihan, Costantino Pitzalis, Douglas J. Veale and Ursula Fearon

J Immunol 2010; 184:6427-6437; Prepublished online 30 April 2010;
doi: 10.4049/jimmunol.0902941
http://www.jimmunol.org/content/184/11/6427

The Journal of Immunology is published twice each month by
The American Association of Immunologists, Inc.,
1451 Rockville Pike, Suite 650, Rockville, MD 20852

Print ISSN: 0022-1767 Online ISSN: 1550-6606.

Acute Serum Amyloid A Induces Migration, Angiogenesis, and Inflammation in Synovial Cells In Vitro and in a Human Rheumatoid Arthritis/SCID Mouse Chimera Model

Mary Connolly,*,† Alessandra Marrelli,‡ Mark Blades,‡ Jennifer McCormick,*,† Paola Maderna,† Catherine Godson,† Ronan Mullan,*,† Oliver FitzGerald,*,† Barry Bresnihan,*,† Costantino Pitzalis,‡ Douglas J. Veale,*,† and Ursula Fearon*,†

Serum amyloid A (A-SAA), an acute-phase protein with cytokine-like properties, is expressed at sites of inflammation. This study investigated the effects of A-SAA on chemokine-regulated migration and angiogenesis using rheumatoid arthritis (RA) cells and whole-tissue explants in vitro, ex vivo, and in vivo. A-SAA levels were measured by real-time PCR and ELISA. IL-8 and MCP-1 expression was examined in RA synovial fibroblasts, human microvascular endothelial cells, and RA synovial explants by ELISA. Neutrophil transendothelial cell migration, cell adhesion, invasion, and migration were examined using transwell leukocyte/monocyte migration assays, invasion assays, and adhesion assays with or without anti–MCP-1/anti–IL-8. NF-κB was examined using a specific inhibitor and Western blotting. An RA synovial/SCID mouse chimera model was used to examine the effects of A-SAA on cell migration, proliferation, and angiogenesis in vivo. High expression of A-SAA was demonstrated in RA patients ($p < 0.05$). A-SAA induced chemokine expression in a time- and dose-dependent manner ($p < 0.05$). Blockade with anti-scavenger receptor class B member 1 and lipoxin A4 (A-SAA receptors) significantly reduced chemokine expression in RA synovial tissue explants ($p < 0.05$). A-SAA induced cell invasion, neutrophil–transendothelial cell migration, monocyte migration, and adhesion (all $p < 0.05$), effects that were blocked by anti–IL-8 or anti–MCP-1. A-SAA–induced chemokine expression was mediated through NF-κB in RA explants ($p < 0.05$). Finally, in the RA synovial/SCID mouse chimera model, we demonstrated for the first time in vivo that A-SAA directly induces monocyte migration from the murine circulation into RA synovial grafts, synovial cell proliferation, and angiogenesis ($p < 0.05$). A-SAA promotes cell migrational mechanisms and angiogenesis critical to RA pathogenesis. ***The Journal of Immunology*****, 2010, 184: 6427–6437.**

Acute-phase serum amyloid A (A-SAA) is an acute-phase protein of the apoprotein family (1, 2). A-SAA is the precursor of insoluble amyloid deposited in the heart, blood vessels, and major organs in secondary amyloidosis and is associated with chronic inflammatory disease, such as rheumatoid arthritis (RA) (3). A-SAA, like many acute-phase proteins, is primarily synthesized by hepatocytes. Secreted A-SAA associates with high-density lipoprotein (HDL), displacing apolipoprotein AI (Apo-AI) and yielding lipoprotein fractions, including SAA, lipid-poor Apo-AI, and lipoprotein-free SAA (4, 5). Persistently high SAA usually indicates reduced Apo-AI and HDL cholesterol as a result of increases in HDL metabolism (5). However, during the acute-phase response, serum levels of A-SAA increase up to 1000-fold, saturating HDL and allowing lipid-free A-SAA to circulate. Extrahepatic production of A-SAA has been implicated in the pathogenesis of chronic diseases, including RA and Alzheimer's disease (6, 7). Additionally, A-SAA is expressed in cholesterol-laden atherosclerosis plaques accumulating in monocyte-derived foam cells within the vascular wall (8). Atherosclerotic cardiovascular disease is the primary cause of premature death in patients with RA (9, 10).

RA is an autoimmune disease characterized by a hyperplastic synovial tissue (ST) capable of destroying articular cartilage and bone. Angiogenesis, the formation of new blood vessels from existing vessels, is a critical early event in inflammation (11), facilitating leukocyte migration from the peripheral blood, which results in a persistent infiltration of predominantly monocyte/macrophage cells into the inflamed joint. These processes are mediated by increased adhesion molecules, chemokines, and matrix metalloproteinases (MMPs). We previously reported increased expression of A-SAA and its receptor in RA ST (7). We and other investigators demonstrated that A-SAA induces adhesion molecule expression, angiogenesis, and MMPs in vitro (12–14). A-SAA has a high affinity for the extracellular matrix components laminin and fibronectin and was shown to enhance leukocyte binding to extracellular matrix through a β1-integrin–dependent mechanism (15, 12). Additionally, A-SAA has two known receptors, lipoxin A_4 (LXA4) receptor/*N*-formyl peptide receptor-like-1 (FPRL-1) and scavenger receptor class B member 1 (SR-B1; formerly CD36 and LIMPII analogous-1), both expressed in RA ST (16). More

*Dublin Academic Medical Centre and †Conway Institute of Biomolecular and Biomedical Research, University College Dublin, Dublin, Ireland; and ‡Department of Experimental Medicine and Rheumatology, William Harvey Research Institute, Barts and The London School of Medicine and Dentistry, London, United Kingdom

Received for publication September 4, 2009. Accepted for publication March 25, 2010.

This work was supported by funding from the Science Foundation of Ireland.

Address correspondence and reprint requests to Dr. Ursula Fearon, St. Vincent's University Hospital, Dublin Academic Medical Centre, Dublin 4, Ireland. E-mail address: ursula.fearon@ucd.ie

Abbreviations used in this paper: Apo-AI, apolipoprotein AI; A-SAA, serum amyloid A; EC, endothelial cell; EGM, endothelial growth medium; FPRL-1, *N*-formyl peptide receptor-like-1; HDL, high-density lipoprotein; HMEC, human microvascular endothelial cell; hpf, high-power field; LXA4, lipoxin A4; MMP, matrix metalloproteinase; NAC, *N*-acetyl-L-cysteine; OA, osteoarthritis; PsA, psoriatic arthritis; RA, rheumatoid arthritis; RASFC, rheumatoid arthritis synovial fibroblast; SF, synovial fluid; SFC, synovial fibroblast; SR-B1, scavenger receptor class B member 1; ST, synovial tissue.

www.jimmunol.org/cgi/doi/10.4049/jimmunol.0902941

recently, it was demonstrated that the effects of A-SAA might also be mediated through TLR2 (17). Its rapid induction during inflammation, localized expression at inflammatory sites, and ability to induce many proinflammatory processes suggest that A-SAA may be directly involved in the pathogenesis of inflammatory joint disease.

In this study, we examined the biological effects of A-SAA on chemokine expression, transendothelial cell migration, monocyte adhesion/migration, and cell invasion using RA synovial fibroblasts (RASFCs), human microvascular endothelial cells (HMECs), and RA whole-tissue synovial explant cultures. We investigated the signaling pathways involved, and, using a human RA synovial/SCID chimera model, examined for the first time in vivo the effects of A-SAA on the induction of monocyte migration from the murine circulation into RA synovial grafts and on synovial cell proliferation and angiogenesis.

Materials and Methods

Arthroscopy and sample collection

RA and psoriatic arthritis (PsA) patients with clinically active inflamed knees prior to biologic therapy, along with osteoarthritis (OA) patients, were recruited from rheumatology outpatient clinics at St. Vincent's University Hospital, Dublin. Serum and synovial fluid (SF) were collected from 48 patients (28 RA and 20 PsA). The median age was 53 y (range, 19–82 y), and 72% of patients were female. All patients had clinically active disease, as evidenced by a hot swollen knee joint, an increased erythrocyte sedimentation rate of 30.5 mm/h (range, 2–100 mm/h), and an increased C-reactive protein of 18 mg/l (range, 4–152 mg/l). All patients had an inadequate response to disease-modifying antirheumatic drug therapy (methotrexate, salazopyrin, hydroxychloroquine, or steroids). Matched ST of an inflamed knee joint was obtained in 33 patients at arthroscopy. Following approval by the institutional ethics committee, all patients gave written informed consent, prior to a day-case arthroscopy procedure under local anesthesia. Using a 2.7-mm-diameter needle telescope (Stortz, Tuttlingen, Germany), biopsies of inflamed synovial membrane were obtained under direct visualization, as previously described (18). Synovial biopsies were snap-frozen and stored at −80°C for protein or mRNA analysis. For SCID mice transplantation experiments, RA synovial biopsies were frozen in a mixture of 40% heat-inactivated FBS, 10% DMSO, and 50% RPMI 1640 tissue culture media. Biopsies were stored in liquid nitrogen until engraftment, as previously described (19).

A-SAA and FPRL-1 mRNA extraction and purification. Total RNA was extracted from cells using RNeasy total RNA isolation protocol (Qiagen, Crawley, U.K.). RNA extraction from synovial biopsies was performed by pooling two biopsies for each patient and adding 200 μl TRIzol reagent (Invitrogen, Dublin, Ireland). The tissue was homogenized using a mortar and pestle (Kimble Chase, Scherf, Germany), and 40 μl chloroform was added. The solution was vortexed briefly and mixed with 70% ethanol in a 1:1 ratio. The mixture was added to a mini column, and total RNA isolation was carried out per the manufacturer's protocol. RNA quality was assessed by spectrophotometry, and samples with a 260:280-nm ratio ≥1.8 were used in subsequent experiments. Isolated RNA was stored at −80°C.

A-SAA and FPRL-l mRNA analysis. Total RNA (1 μg) from synovial biopsy was reverse transcribed to cDNA. FPRL-1 and GAPDH Quantitect Primer Assays were used for the quantification of cDNA. These assays consist of specific forward and reverse primers derived from gene sequences contained in the National Center for Biotechnology Information Reference Sequence database (www.ncbi.nlm.nih.gov/RefSeq) and amplified 90- and 96-bp products, respectively. Relative quantification of gene expression was performed with preoptimized conditions using Lightcycler PCR technology (Roche Diagnostics, Lewes, U.K.). PCRs were performed in duplicate using 10 μl 2× Quantitect SYBR Green PCR Master Mix, 2 μl Quantitect Primer Assay, 2 μl cDNA, and 6 μl nucleotide-free H_2O to yield a 20-μl reaction. Specific primers for A-SAA were used to amplify a 335-bp A-SAA product: sense primer (5′-AAG CTT CTT TCC GTT CCT TGG-3′) and antisense primer (5′-GAG AGC AGA GTG AAG AGG AAG C-3′). After preincubation (94°C, 10 min), each PCR sample underwent a 35-cycle amplification regimen of denaturation (94°C, 1 min), primer annealing (60–56°C, 1 min), and extension (72°C, 1 min) in a thermal cycler (MJ Research, Cambridge, MA). Ethidium bromide staining of 2.5% agarose gels was used to detect generated PCR products. All gels were visualized using the Eagle Eye II still video system (Stratagene, Amsterdam, The Netherlands).

Acute A-SAA measurement by ELISA. A-SAA protein levels were measured using a sandwich enzyme immunoassay, as per the manufacturer's protocol (Biosource, London, U.K.). Serum, SF, human ST explant culture supernatants, and protein lysates were assayed. For synovial protein lysates, biopsies were snap-frozen and homogenized using a Mikro-Dismembrator (B. Braun Biotech International, Allentown, PA). The absorbance was measured at 405 nm. Standards ranged from 9.4–300 ng/ml. The minimal detectable level of A-SAA was 5 ng/ml.

Isolation and culture of RA fibroblast-like synoviocytes. Synovial biopsies were digested with 1 mg/ml collagenase type 1 (Worthington Biochemical, Freehold, NJ) in RPMI 1640 (Life Technologies-BRL, Paisley, U.K.) for 4 h at 37°C in humidified air with 5% CO_2. Dissociated cells were grown to confluence in RPMI 1640, 10% FCS (Life Technologies-BRL), 10 ml 1 mmol/l HEPES (Life Technologies-BRL), penicillin (100 U/ml; Bio-Sciences, Dublin, Ireland), streptomycin (100 U/ml; Bio-Sciences), and fungizone (0.25 μg/ml; Bio-Sciences) before passaging. Cells were used between passages four and eight. K4 cells, an immortalized human healthy donor synoviocyte cell line, were cultured as per RASFCs and used between passages 35 and 38.

HMECs

HMECs (Lonza Wokingham, Berkshire, U.K.) were incubated in cell basal medium supplemented with endothelial growth medium (EGM)-microvascular bullet kit containing 25 ml FCS, 0.5 ml human epidermal growth factor, 0.5 ml hydrocortisone, 0.5 ml gentamicin, and 0.5 ml bovine brain extract, as previously described (14).

Measurement of IL-8 and MCP-1 in RASFCs and HMECs. To assess the effects of A-SAA on chemokine expression, RASFCs and HMECs were stimulated with A-SAA, and IL-8 and MCP-1 production was quantified. A-SAA was purchased from PeproTech (Rocky Hill, NJ). Endotoxin levels ≤ 1 EU in A-SAA preparations were confirmed by *Limulus* assay (Bio-Whittaker, Walkersville, MD). RASFCs or HMECs were plated to a density of 12×10^4 in 96-well plates for 48 h in medium plus supplements, followed by stimulation with A-SAA (10 or 50 μg/ml) for 24 h. Additionally, RASFCs were stimulated with A-SAA (10 or 50 μg/ml), IL-1β (10 ng/ml), or TNF-α (10 ng/ml) for 3, 6, 12, 24, or 48 h. Supernatants were harvested, and protein levels of IL-8 and MCP-1 were measured by ELISA (R&D Systems, Abingdon, U.K.), according to the manufacturer's protocol.

RA ST explant culture

To examine the spontaneous release of A-SAA from active ST, we established an ex vivo ST explant model that maintains the synovial architecture and cell–cell contact and, therefore, more closely reflects the in vivo environment. Synovial explant tissue was sectioned into 3-mm cubes and cultured immediately from arthroscopy (to maintain maximal activity) in 96-well plates (Falcon, Franklin Lakes, NJ) in RPMI 1640, supplemented with streptomycin (100 U/ml) and penicillin (100 U/ml), for 24 h at 37°C in 5% CO_2. Spontaneous release of A-SAA following the 24-h culture of synovial biopsies from RA (n = 22) and PsA (n = 11) patients (all with active knee involvement, prior to biologic therapy) was measured by ELISA (Biosource). Additional experiments examined the direct effect of A-SAA on cultured RA and PsA synovial explant cultures. Explants were serum starved for 24 h, to allow quiescence of the tissue, and then stimulated with A-SAA (10 or 50 μg/ml), IL-1β (10 ng/ml), or TNF-α (10 ng/ml) for 24 h and over a 3–48-h time course. Supernatants were harvested and assayed for IL-8 and MCP-1 by ELISA (R&D Systems).

SR-B1 and FPRL-1 blockade

To investigate the effect of blocking the proinflammatory effects of endogenously produced A-SAA, RA explants (n = 6) were cultured in the presence of inhibitors to two A-SAARs: SR-B1 and FPRL-1. RA ST biopsies were sectioned, as described above, and cultured immediately from arthroscopy (to maintain maximal active endogenous production) in RPMI 1640 in the presence of mouse anti–SR-B1 (10 μg/ml, clone 25/CLA-1; BD Biosciences, Oxford, U.K.) or 10 μg/ml isotype-matched mouse IgG1 control (clone 11711, R&D Systems), LXA4 (5(*S*)-6(*R*)-15(*S*)-trihydroxy-7,9,13-*trans*-11-*cis*-eicosatetraenoic acid) (1 nM, BIOMOL, Plymouth Meeting, PA), or ethanol vehicle control for 24 h. Explant supernatants were harvested and assayed for IL-8 and MCP-1 by ELISA.

Isolation of PBMCs and neutrophils

PBMCs were isolated from normal donors, as previously described (14). Human neutrophils were purified from normal donors and RA patients by dextran sedimentation and Ficoll gradient centrifugation, followed by hypotonic lysis of contaminating erythrocytes. Neutrophils were resuspended in 1% EGM prior to experiments.

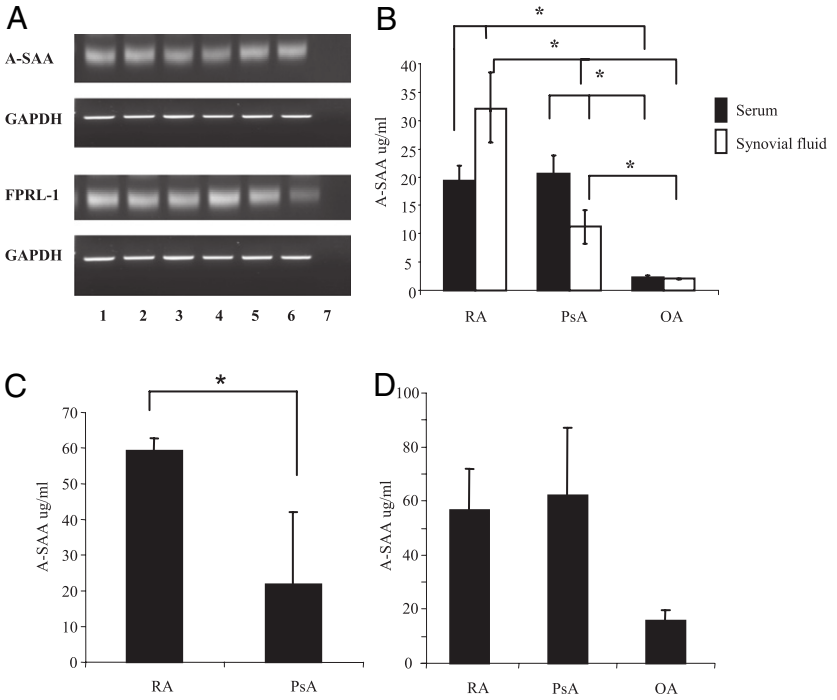

FIGURE 1. A-SAA expression in patients with inflammatory arthritis. A-SAA and FPRL-1 mRNA expression in ST lysates. *A*, A-SAA and FPRL-1 are expressed in ST lysates of RA (*lanes 1, 2*), PsA (*lanes 3, 4*), and OA (*lanes 5, 6*) patients. *Lane 7* shows negative control. *B*, A-SAA protein levels were significantly higher in matched serum and SF from RA ($n = 28$) and PsA ($n = 20$) patients compared with OA patients ($n = 5$), and the production of A-SAA was significantly higher in RA SF compared with PsA SF. *C*, Spontaneous release of A-SAA protein from cultured biopsies is higher from RA tissue explants ($n = 22$) compared with PsA explants ($n = 11$). *D*, A-SAA protein levels in ST lysates are similar in RA ($n = 13$) and PsA ($n = 11$) tissues but higher than OA ($n = 6$). Values are expressed as mean ± SEM. $*p < 0.05$.

Monocyte migration and neutrophil transendothelial assays

Monocyte transwell migration chambers, with a pore size of 5 μm (Cell Biolabs, San Diego, CA), were used to examine the effect of A-SAA on monocyte migration. A-SAA (10 or 50 μg/ml) was added to the lower compartment in 150 μl media. Approximately 1×10^6 monocytes in 0.1 ml were added to the top chamber and incubated at 5% CO_2 at 37°C for 4 h. Cells that had migrated to the lower compartment were counted using a hemocytometer. The effect of A-SAA on the transendothelial migration of neutrophils was performed using transculture chambers with a pore size of 3 μm (BD Biosciences). Approximately 100,000 HMECs were seeded onto fibronectin-coated 24-well chambers, with a pore size of 3 μm (BD Biosciences), and grown to a confluent monolayer in 5% CO_2 at 37°C. A-SAA (10 or 50 μg/ml), IL-1β (10 ng/ml), or TNF-α (10 ng/ml) was added to the lower compartment; 1×10^6 neutrophils in 0.1 ml were added to the HMEC monolayer for 2–48 h. Cells that had migrated to the lower compartment were counted using a hemocytometer. To assess the role of IL-8, cells were pretreated with 2.5 μg/ml human anti–IL-8 IgG1 mAb (clone 6217) (R&D Systems) and isotype-matched IgG1 control (2.5 μg/ml) for 1 h.

Transwell invasion assay

Biocoat Matrigel Invasion Chambers (BD Biosciences) were used to assess EC migration in response to A-SAA, IL-1β, and TNF-α. Cells were seeded at a density of 2.5×10^4 per well in the migration chamber on 8-μm membranes precoated with Matrigel. EGM containing A-SAA (10–50 μg/ml), IL-1β (10 ng/ml), or TNF-α (10 ng/ml) was placed in the lower well of the assay. Cells were allowed to migrate for 24 h in EGM media containing 1% FCS. Nonmigrating HMECs were removed from the upper surface by gentle scrubbing. Migrating cells attached to the lower membrane were fixed with 1% glutaraldehyde and stained with 0.1% crystal violet. To assess the average number of migrating cells, cells were counted in five random high-power fields (hpfs).

PBMC adhesion assay

We previously demonstrated that A-SAA could induce adhesion of PBMCs to HMECs; in this study, we examined whether A-SAA–induced adhesion is mediated by MCP-1. HMECs were grown to confluence in 12-well plates and stimulated with A-SAA and TNF-α for 6 h. Following stimulation, cells were washed twice with PBS and incubated for 1 h with 1 ml serum-free RPMI 1640 containing PBMCs at a density of 0.5×10^6 cells. Nonadherent cells were removed by washing with sterile PBS. Adhesion was measured by counting HMEC-bound PBMCs from five random fields (×40 magnification) per duplicate well. For PBMC adhesion blockade, PBMCs were incubated with 10 μg/ml human anti–MCP-1 IgG1 mAb (clone 24822; R&D Systems) or IgG1 isotype-matched control overnight.

Inhibition of A-SAA–induced IL-8 and MCP-1 expression by N*-acetyl-*L*-cysteine.* To assess the role of NF-κB in A-SAA signaling pathways, experiments assessing the effects of A-SAA–induced IL-8 and MCP-1 expression were performed, as above, in the presence or absence of inhibitors to the p38 MAPK pathway (SB203580) and the NF-κB pathway (*N*-acetyl-L-cysteine [NAC]; both purchased from Calbiochem, Merck Chemicals, Nottingham, U.K.). Cell viability studies using ethidium bromide-acridine orange uptake showed that >95% of cells remained viable, demonstrating that the inhibitors were not cytotoxic. RA ST explant cultures were pretreated with SB203580 (10 μM) and NAC (10 mM) for 24 h in the presence or absence of A-SAA, IL-1β, and TNF-α. Supernatants were harvested, and IL-8 and MCP-1 levels were analyzed by ELISA.

Analysis of NF-κB. RA ST explants and HMECs were incubated with A-SAA (10 μg/ml) or TNF (10 ng/ml) for 15 min. Following incubation, cell lysates were separated by SDS-PAGE and transferred onto nitrocellulose membranes. Western blotting using primary rabbit polyclonal Ab NF-κB (Upstate Biotechnology, Lake Placid, NY) was performed according to the manufacturers' protocol. Blots were developed using ECL (Pierce, Rockford, IL) for detection of HRP. NF-κB nuclear translocation in RA fibroblast-like synoviocytes was detected by immunofluorescence. Cells grown in eight-chamber culture slides (BD Biosciences) were incubated with A-SAA (10 μg/ml) for 15 min and then washed in PBS. Cells were fixed in 4% paraformaldehyde for 20 min and blocked in 1% casein solution for 20 min. Incubations were performed with rabbit polyclonal anti–NF-κB p65 (1:100; Santa Cruz Biotechnology, Santa Cruz, CA) for 1 h and then with Cy3 (1:500 dilution; Sigma-Aldrich, St. Louis, MO) for 30 min. Slides were washed in PBS, mounted with Antifade (Molecular Probes, Eugene, OR), and assessed by immunofluorescence microscopy (×40 magnification).

U937 labeling and migration into human synovium transplanted onto SCID mice. U937 human myelomonocytic cell lines were cultured in RPMI 1640 medium plus 10% FCS. Cells were subcultured and maintained at a concentration of $0.5–1.0 \times 10^6$ cells/ml, as previously described (20). Briefly, U937 cells were washed and incubated with CellTracker Orange dye (Invitrogen) at 37°C at a concentration of 5 μg dye per 20×10^6 cells in 15 ml RPMI 1640 for 30 min. Cells were washed, and the working solution was replaced with fresh prewarmed RPMI 1640 plus 10% FCS and incubated at 37°C for 30 min. Finally, cells were washed twice to remove unbound dye and resuspended in 0.9% saline at a cell concentration of 50×10^6 cells/ml for i.v. injection. Cell viability was determined via trypan blue exclusion and was always >90%. Labeling efficiency was confirmed before transplantation by examining a wet preparation of labeled cells under the ultraviolet microscope.

RA ST biopsies were thawed from liquid nitrogen immediately before surgery, washed in saline, and kept in saline-moistened sterile gauze over ice. Beige SCID mice were anesthetized, and biopsies were inserted s.c. in the dorsal skin overlying the scapulae (two per mouse). Fourteen days

posttransplantation, animals were injected intragraft with PBS + 0.1% BSA, TNF-α, or A-SAA; immediately thereafter, 100 μl the labeled U937 (5×10^6 cells/animal) was injected into the tail vein. Mice were culled 48 h postinjection, and tissues were harvested for histological examination. Migration of U937 cells into grafts was assessed histologically by ultraviolet fluorescence microscopy.

Quantification of cell migration into grafts. RA ST grafts were embedded in OCT compound, snap-frozen in liquid nitrogen, and stored at −80°C. Serial cryosections (5 μm) were cut, mounted, and air-dried overnight. Immunofluorescent analysis sections were fixed in acetone for 10 min and immunostained for CD68 using a species-specific MAb (Dako, Dublin, Ireland) and Alexa 488-conjugated polyclonal secondary Ab (Invitrogen). Each transplant was sectioned, three cutting levels were analyzed (200 μm per level) and digitized, and the migration of cells from the murine circulation to grafts was assessed as the number of double-positive (red/green) cells/hpf. Forty hpfs/transplant were analyzed, and the results are expressed as the number of double-positive cells/hpf, as previously described (21).

Immunohistochemical expression of factor VIII and proliferation marker Ki67

Grafted ST sections were fixed in acetone for 10 min, incubated with primary Abs against mouse monoclonal factor VIII and Ki67 (DakoCytomation) at 37°C, and stained using a routine three-stage immunoperoxidase technique incorporating avidin-biotin-immunoperoxidase complex (DakoCytomation). An irrelevant isotype-matched MAb was negative control. Color was developed in solution containing diaminobenzadine-tetrahydrochloride (Sigma-Aldrich), 0.5% H_2O_2 in PBS buffer (pH 7.6). Slides were counterstained with hematoxylin and mounted. Ki67 was assessed by quantifying the number of positive-staining cells/hpf. Factor VIII was assessed by quantifying the number of blood vessels/hpf (five hpfs were counted/transplant), as previously described (20, 21).

Statistical analysis. Data are expressed as the mean ± SEM. Statistical analysis was performed using SPSS 11 for Windows (SPSS, Chicago, IL). Comparisons between treated and untreated ST and RASFCs were made using the Wilcoxon signed-rank test for paired values. The Student *t* test was used to analyze parametric data. A p value <0.05 was considered significant.

Results

A-SAA gene and protein expression in serum, SF, and ST

Real-time PCR analysis of total RNA was used to examine A-SAA and its receptor FPRL-1 mRNA expression in ST from patients with inflammatory arthritis (n = 6). A-SAA and FPRL-1 gene expression was detected in all six ST samples analyzed, with similar levels of expression seen in RA (n = 2), PsA (n = 2), and OA (n = 2) tissue (Fig. 1*A*); no gene expression was observed in the negative controls. Serum and SF A-SAA levels were significantly higher in RA and PsA patients compared with OA patients ($p < 0.05$) (Fig. 1*B*) and healthy controls (4.9 ± 1.85 μg/ml; $p < 0.05$). Levels of A-SAA in RA SF (32.04 ± 5.92 μg/ml) were significantly higher than in matched serum (19.41 ± 2.63 μg/ml; $p = 0.05$), suggesting localized A-SAA production in the inflammatory joint. In addition, the levels of SAA were significantly higher in RA SF compared with PsA SF ($p = 0.014$). Conversely, levels of A-SAA in PsA sera (20.62 ± 3.2 μg/ml) were significantly higher than in PsA SF (11.24 ± 2.92 μg/ml; $p = 0.04$) suggesting differential systemic and localized expression of A-SAA in PsA versus RA. In this study, we also measured A-SAA protein levels in primary RASFCs, normal synovial fibroblasts (SFCs), and RA and healthy control neutrophils. We demonstrated higher levels of SAA in RASFCs (67.73 ± 8.07 ng/ml) versus normal SFCs (38.44 ± 2.16 ng/ml) and in RA neutrophils (87.03 ± 8.38 ng/ml) compared with healthy controls (18.67 ± 1.7 ng/ml).

We established an ex vivo ST culture model to examine expression levels of A-SAA in the joint. This culture model involves many cell types maintaining the synovial architecture and cell–cell contact of the tissue. To examine endogenous production, explants were cultured immediately from arthroscopy to maintain the active environment of the joint. Endogenous A-SAA levels in

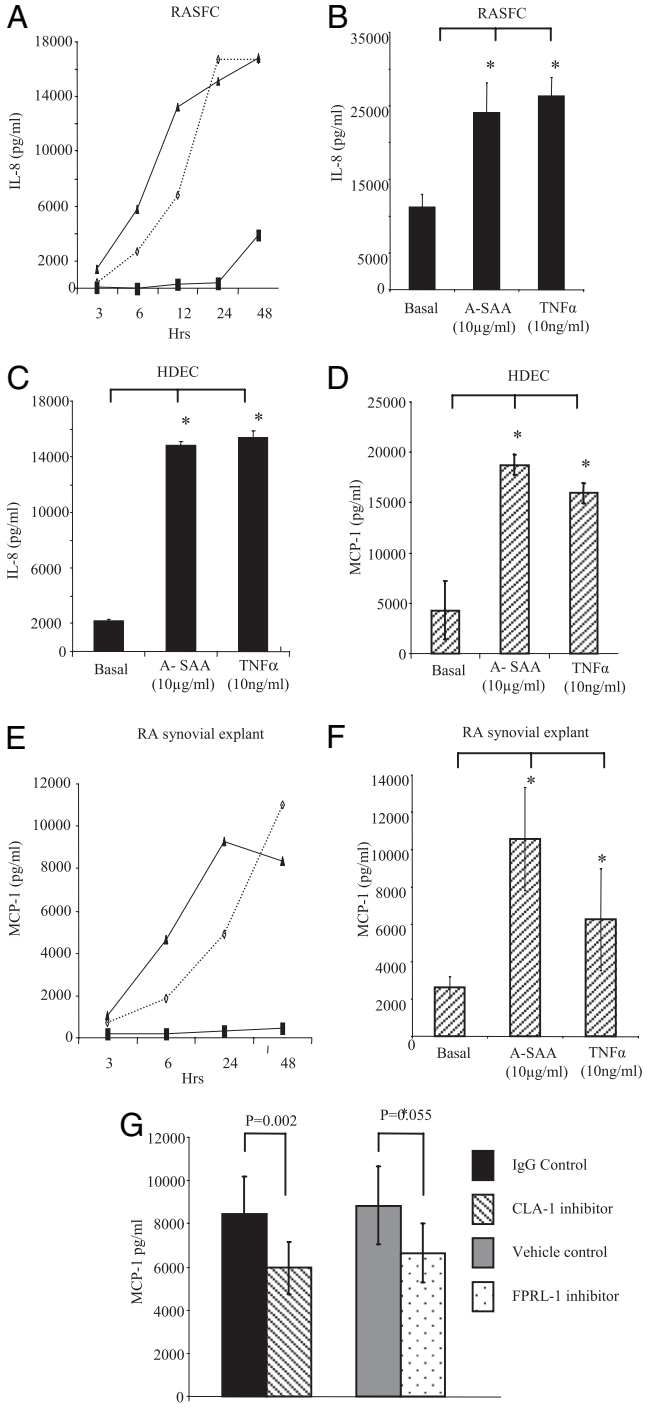

FIGURE 2. A-SAA stimulates IL-8 and MCP-1 from RASFCs, HMECs, and RA synovial explants. *A*, Stimulation of human RASFCs (n = 6) with A-SAA at 10 and 50 μg/ml for the indicated time periods: basal (■), A-SAA 10 μg/ml (♦), and A-SAA 50 μg/ml (▲). A-SAA increased IL-8 protein levels from cultured RASFCs over 3–48 h, with maximum expression observed between 12 and 48 h. Increased IL-8 protein levels following 24-h stimulation with A-SAA (10 μg/ml) and TNF-α (10 ng/ml) from cultured RASFCs (n = 6) (*B*) and HMECs (n = 3) (*C*). *D*, MCP-1 protein production following 24-h stimulation with A-SAA (10 μg/ml) and TNF-α (10 ng/ml) from HMECs is also upregulated (n = 3). *E*, A-SAA (10–50 μg/ml) increased MCP-1 expression from RA ST cultures over 3–48 h, with maximum levels observed between 24 and 48 h. *F*, Increased MCP-1 expression following 24-h stimulation of RA ST cultures (n = 6) by A-SAA (10 μg/ml) showed an effect comparable to stimulation with TNF-α (10 ng/ml). *G*, SR-B1 and FPRL-1 inhibition significantly reduces MCP-1 production in RA synovial explant tissue (n = 6). Values are expressed as the mean ± SEM of replicate experiments. $*p < 0.05$, compared with basal control.

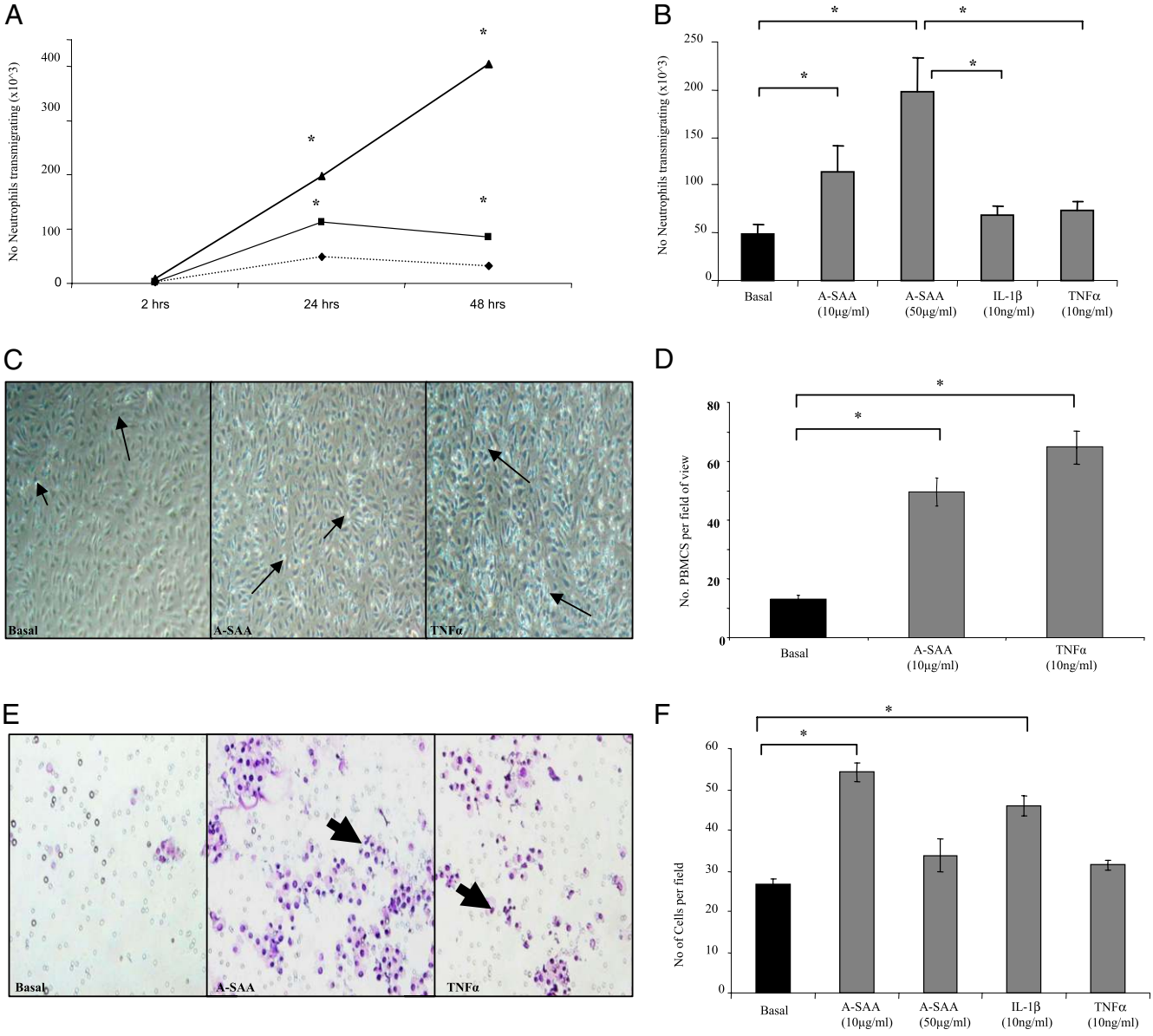

FIGURE 3. A-SAA induces leukocyte recruitment, PBMC adhesion, and EC invasion. HMEC monolayers grown in transculture chambers were cocultured with human neutrophils. A-SAA (10 or 50 μg/ml), IL-1β (10 ng/ml), or TNF-α (10 ng/ml) was added to lower wells. *A*, A-SAA induced neutrophil transendothelial cell migration over 2–48 h. Basal (■), A-SAA10 μg/ml (♦), and A-SAA 50 μg/ml (▲). *B*, Bar graph demonstrating that A-SAA significantly induces transmigration compared with control at 24 h ($n = 6$). *C*, Representative photomicrographs of PBMC:HMEC adhesion following A-SAA (50 μg/ml) or TNF-α (10 ng/ml) stimulation for 6 h. Arrows point to monocyte cells adhering to EC monolayer (original magnification ×20). *D*, Bar graph representing PBMC:HMEC adhesion quantification following stimulation with A-SAA and TNF-α ($n = 4$). *E*, Representative photomicrograph shows HMEC invasion (arrows) following stimulation with A-SAA (10 μg/ml) or TNF-α (10 ng/ml). At 24 h, invading cells attached to the lower membrane were fixed (1% glutaraldehyde) and stained (0.1% crystal violet) (original magnification ×40). *F*, Representative bar graph quantifying HMEC invasion ($n = 4$) following A-SAA (10, 50 μg/ml), IL-1β, or TNF-α (10 ng/ml) stimulation. All values are expressed as mean ± SEM of replicate experiments. $*p < 0.05$, compared with basal control.

synovial explant cultures were significantly higher in RA patients compared with PsA patients (59.2 ± 20.34 μg/ml versus 21.7 ± 3.51 μg/ml; $p < 0.05$) (Fig. 1*C*). A-SAA levels quantified in ST lysates from patients with RA ($n = 13$), PsA ($n = 11$), and OA ($n = 6$) were similar in RA and PsA patients (56.89 ± 15 μg/ml versus 61.96 ± 23.33 μg/ml, respectively) and were markedly higher than in OA patients (15.9 ± 4.0 μg/ml) (Fig. 1*D*).

IL-8 and MCP-1 responses to A-SAA from RASFCs, HMECs, and RA synovial explants

To determine whether A-SAA directly induces chemokine secretion in inflammatory cells, the expression of proinflammatory chemokines IL-8 and MCP-1 in response to stimulation by A-SAA was assessed on RASFCs, HMECs, and RA synovial explant cultures. A-SAA increased IL-8 expression in RASFCs over 3–48 h (Fig. 2*A*). A-SAA increased IL-8 expression as early as 3 h, compared with control, from a mean of 132.94 pg/ml to 374.9 and 1,398.13 pg/ml respectively, reaching maximum levels between 24 and 48 h (16,672.68 pg/ml and 16,814.17 pg/ml, respectively) compared with control (381.06 and 3,830.03 pg/ml, respectively). Similar induction of IL-8 was observed following IL-1β and TNF-α stimulation to a maximum of 9,436.29 and 18,393.09 pg/ml at 48 h. The effect of A-SAA on IL-8 expression in RASFCs ($n = 6$) was examined following 24 h of stimulation (Fig. 2*B*). A-SAA significantly increased IL-8 production compared with unstimulated cells ($p < 0.05$), an effect similar to stimulation with

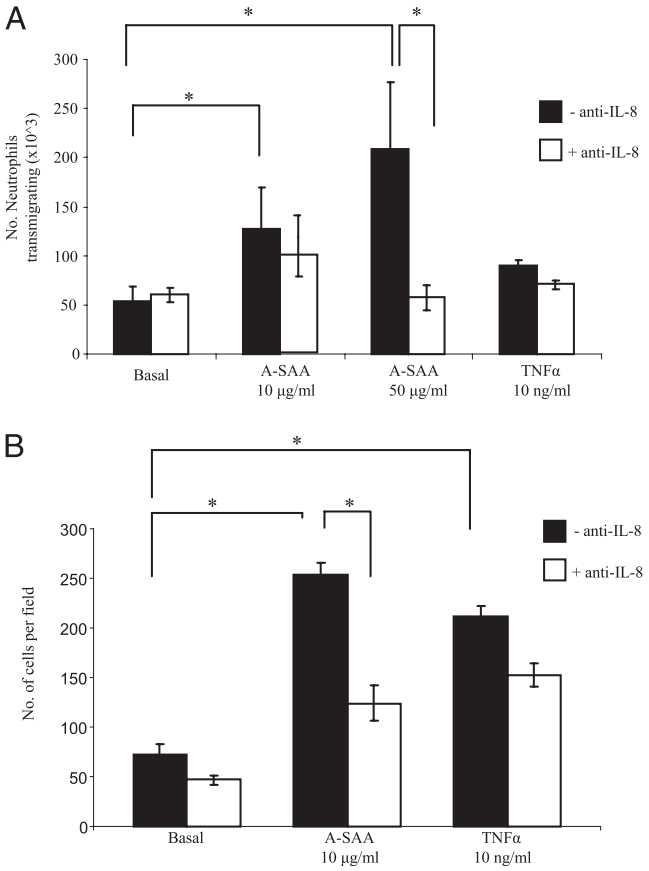

FIGURE 4. A-SAA induces leukocyte recruitment and PBMC adhesion via IL-8 and MCP-1. *A*, A-SAA–induced neutrophil transendothelial cell migration is significantly reduced by preincubation with anti–IL-8 Ab. Results are expressed as the mean ± SEM of the number of neutrophils transmigrating ($\times 10^3$) in three experiments. *B*, A-SAA–induced PBMC: HMEC adhesion is significantly reduced by preincubation with anti–MCP-1 Ab. Results are expressed as the mean ± SEM of the number of cells per hpf ($n = 3$ experiments). $*p < 0.05$.

TNF-α ($p < 0.05$). Additionally, A-SAA significantly induced MCP-1 expression in RASFCs from a basal level of 1933.56 ± 75.01 pg/ml to 5892.31 ± 755.32 and 8489.58 ± 817.05 pg/ml following stimulation with 10 and 50 μg/ml, respectively ($p < 0.05$). Additionally, stimulation with IL-1β and TNF-α resulted in significant increases in MCP-1 expression (6578.683 ± 428.75 pg/ml and 9035.36 ± 769.02 pg/ml, respectively; $p < 0.05$). In HMEC cultures, A-SAA significantly induced MCP-1 and IL-8 expression ($p < 0.05$), an effect similar to that of TNF-α (Fig. 2*C*, 2*D*).

Fig. 2*E* illustrates the effect of A-SAA on MCP-1 production from a representative RA synovial explant culture over a time course of 3–48 h. A-SAA (10 and 50 μg/ml) increased MCP-1 expression at 3 h, reaching maximum levels between 24 and 48 h (Fig. 2*E*). Stimulation with IL-1β and TNF-α increased MCP-1 expression, reaching maximum levels at 24 h, from a control level of 398.83 pg/ml to 6193.13 pg/ml (IL-1β) and 5072.31 pg/ml (TNF-α). Similar effects of A-SAA on IL-8 were observed over a 3–24-h time course (data not shown). Because 24 h was the optimal time point for chemokine response, RA whole-tissue synovial explant cultures ($n = 6$) were stimulated with A-SAA for 24 h (Fig. 2*F*), with MCP-1 expression increasing significantly from control levels of 2,649.1 ± 572.35 pg/ml to 10,562.4 ± 2,756.62 pg/ml (A-SAA 10 μg/ml; $p < 0.05$) and 12,211 ± 2,982.48 pg/ml (A-SAA 50 μg/ml; $p < 0.05$). Similarly, stimulation with TNF-α significantly upregulated MCP-1 expression, although to a lesser degree than A-SAA, to a mean level of 6262.67 ± 2730.08 pg/ml ($p < 0.05$; Fig. 2*F*). Because localized production of A-SAA was different in PsA patients compared with RA patients, we examined the effects of A-SAA on PsA synovial explants; A-SAA had no significant effect on MCP-1 or IL-8 production ($n = 5$). A-SAA (10 μg/ml) induced MCP-1 levels from basal levels of 3,870.3 ± 726.34 pg/ml to 5,265.7 ± 1,092.42 pg/ml (NS), and it induced IL-8 from 121,171.2 ± 22,372.98 pg/ml to 143,202.4 ± 18,748.13 pg/ml (NS). These data demonstrate that A-SAA responses are more specific in RA patients compared with those with PsA.

LXA4, an eicosanoid metabolite with anti-inflammatory actions, was shown to inhibit the proinflammatory actions of A-SAA by competitive binding with FPRL-1 and differential regulation of NF-κB (22). Additionally, recent evidence showed that A-SAA might function through CD36 and LIMPII analogous-1 (SR-B1), a scavenger receptor for the Apo-AI constituent of HDL (16). To assess whether blocking these receptors inhibits endogenous A-SAA–induced proinflammatory events, RA explants were cultured in the presence of mouse anti–SR-B1 (10 μg/ml) versus isotype-matched control (10 μg/ml) and in the presence of LXA4 (1 nM) versus vehicle control. MCP-1 expression in synovial explant tissue (IgG control) was inhibited from 8425.66 pg/ml ± 1719.88 pg/ml to 5959.14 ± 1216.4 pg/ml in the presence of anti-SR-B1 ($p = 0.002$) and from 8833.4 ± 1803.11 pg/ml (ethanol vehicle control) to 6637.38 ± 1354.85 pg/ml in the presence of LXA4 ($p = 0.055$) (Fig. 2*G*). Similarly, SR-B1 blockade significantly inhibited MCP-1 levels from IgG control from 171,450.1 ± 30,874.45 pg/ml to 128,794.3 ± 21,856.77 pg/ml ($p = 0.012$), and LXA4 decreased IL-8 production from 136,903 ± 18,464.89 pg/ml to 115,941.1 ± 18,075.4 pg/ml.

A-SAA induces migration, invasion, and adhesion. Angiogenesis and EC activation are essential steps in the progression of RA; therefore, to further assess the potential role of A-SAA in inducing these processes, we examined neutrophil transendothelial cell migration, EC adhesion, and invasion. A-SAA–induced neutrophil transendothelial cell migration is shown in Fig. 3*A* and 3*B*. A-SAA significantly increased neutrophil transendothelial cell migration in a concentration- and time-dependent manner compared with control ($p < 0.05$), reaching maximum levels of cell migration at 48 h, with 50 μg/ml A-SAA. TNF-α and IL-β increased neutrophil transendothelial migration compared with control cells (control, 49.42 ± 9.14 [$\times 10^3$] versus IL-1β, 68.67 ± 9.42 [$\times 10^3$] and TNF-α, 73.83 ± 9.17 [$\times 10^3$]) after 24 h, although this was not significant (Fig. 3*B*). A-SAA (50 μg/ml)-induced transmigration was significantly higher compared with IL-1β and TNF-α ($p < 0.01$). Additionally, A-SAA (10 and 50 μg/ml) increased monocyte migration from a basal level of 267 ± 34.9 ($\times 10^3$) to 477 ± 73.1 ($\times 10^3$; $p < 0.01$) and 496 ± 51.1 ($\times 10^3$; $p < 0.01$), respectively.

The ability of A-SAA to promote PBMC adhesion to EC monolayers was also examined. Resting PBMCs were incubated on confluent HMEC monolayer cultures pretreated with A-SAA (10 μg/ml) for 24 h. Adhesion was expressed as the number of PBMCs adhering to the HMEC monolayer and was assessed in five hpfs. A-SAA (10 μg/ml) significantly increased PBMC: HMEC adhesion, compared with control stimulation, from a basal ratio of 1 ± 0.1 to 3.8 ± 0.36 ($p < 0.05$; Fig. 3*C*, 3*D*). TNF-α significantly increased PBMC adhesion from a basal ratio of 1 ± 0.1 to 4.97 ± 0.46 ($p < 0.05$).

We then examined the effect of A-SAA on HMEC invasion using transwell Matrigel invasion chambers. HMEC invasion was significantly induced by A-SAA (10 μg/ml) (Fig. 3*E*, 3*F*; $p < 0.01$; $n = 6$). Cell invasion increased by 103% ± 2.21% compared with control, a greater effect than stimulation with TNF-α or IL-1β ($p < 0.05$).

A-SAA–induced migration and adhesion are inhibited by neutralizing IL-8 and MCP-1

Chemokines are important mediators in inflammatory arthritis and play a critical role in inducing the influx of neutrophils, monocytes, and lymphocytes into the synovium at an early stage of disease, resulting in joint destruction. In addition to their chemoattractant effects, some studies suggested that chemokines might mediate other processes, such as angiogenesis, adhesion, or matrix turnover. Therefore, we examined whether A-SAA–induced cell migration and adhesion are mediated by IL-8 and MCP-1. Incubation with anti–IL-8 significantly blocked A-SAA–induced neutrophil transendothelial cell migration at 24 h, demonstrating a functional IL-8 response in HMECs (Fig. 4*A*). No inhibition of SAA-induced transendothelial cell migration was observed in the presence of an IgG-matched isotype control. Additionally, anti–MCP-1 significantly inhibited A-SAA–induced PBMC adhesion ($p < 0.05$; Fig. 4*B*), as well as TNF-α–induced adhesion; however, this was not significant. No inhibition of A-SAA–induced PBMC adhesion was observed in the presence of an IgG-matched isotype control.

A-SAA upregulates IL-8 and MCP-1 via the NF-κB pathway. To determine the possible pathways involved in A-SAA–induced IL-8 and MCP-1 expression in RA ST, we tested different specific signaling inhibitors, including a MAPK p38 inhibitor (SB203580) and an NF-κB inhibitor (NAC). Preincubation with NAC significantly inhibited A-SAA–induced MCP-1 production in RA explant cultures ($p < 0.05$; Fig. 5*A*) and TNF-α stimulation ($p < 0.05$; Fig. 5*B*). Additionally, coincubation of NAC with A-SAA dramatically reduced IL-8 expression in RA explant cultures, although the difference did not reach statistical significance (data not shown). No significant effect was observed with inhibition of p38MAPK. To further demonstrate a specific role for NF-κB in A-SAA signaling in HMECs and RA ST, we examined NF-κB expression by Western blot. Consistent with our previous studies showing IκBα degradation in HMECs (14), A-SAA induced NF-κB expression 15 min following stimulation in RA ST explants (Fig. 5*Di*) and HMECs (Fig. 5*Dii*). Fig. 5*D* shows the quantitative analysis of NF-κBp65 by densitometry, revealing significant induction in response to A-SAA in HMECs and RA synovial explants. Finally, we confirmed that A-SAA induces NF-κB expression in RASFCs by demonstrating translocation of the p65 subunit of NF-κB from the cytoplasm to the nucleus (Fig. 5*E*, 5*F*).

SAA upregulates monocyte migration, angiogenesis, and cell proliferation in the hu-SCID model. To assess the role of A-SAA on monocyte cell migration in vivo, we engrafted RA ST into SCID mice. Fourteen days posttransplantation, grafts were injected with PBS + 0.1% BSA (negative control) or A-SAA (four animals per condition, $n = 8$ grafts). Immediately after intragraft

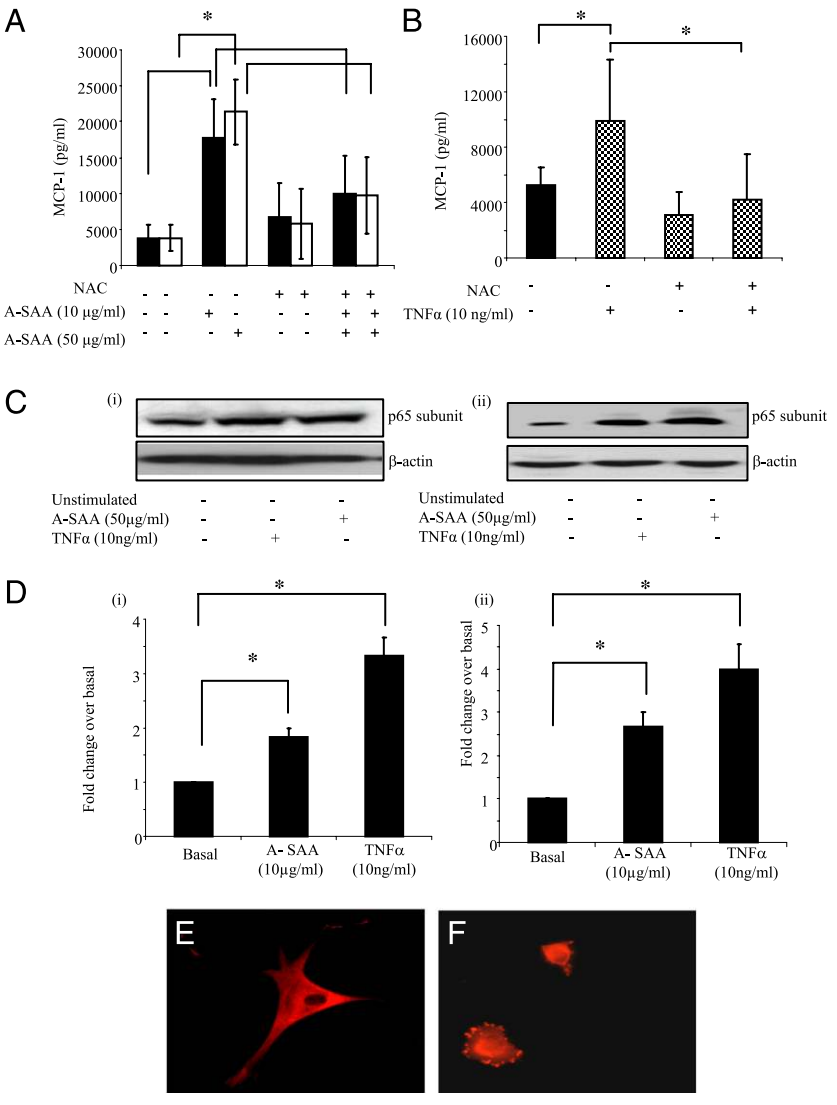

FIGURE 5. A-SAA upregulates chemokine expression via signaling through NF-κB–mediated pathways. RA whole-tissue synovial explant cultures were incubated with NAC, an inhibitor of NF-κB, prior to stimulation with A-SAA (10 or 50 μg/ml) or TNF-α (10 ng/ml). NAC significantly inhibited A-SAA-induced (10 or 50 μg/ml) MCP-1 production by ST (*A*) and stimulation with TNF-α (10 ng/ml) (*B*). Values are expressed as mean ± SEM. $*p < 0.05$. *C*, Representative Western blot demonstrating increased expression of NF-κB in response to A-SAA (10 μg/ml) and TNF-α (10 ng/ml) in RA synovial explant cultures (*i*) and HEMCs (*ii*). *D*, Densitometric analysis of Western blots in RA synovial explant cultures (*i*) and HMECs (*ii*). Immunofluorescence staining of NF-κB p65 on unstimulated RASFCs (*E*, original magnification ×20) and on RASFCs stimulated for 30 min with 50μg/ml of A-SAA (*F*, original magnification ×20).

injection, mice received an i.v. injection of fluorescently labeled U937 cells. Graft cryosections were stained by immunofluorescence for CD68 (LAMP-1). Fig. 6*A* shows representative images, demonstrating that A-SAA increased U937 monocyte migration into RA ST (*right panel*) compared with PBS control (*left panel*). Migrated U937 cells were distinguishable from resident macrophages by CD68 (green fluorescence) and CellTracker Orange dyes (red orange) double positivity, giving a yellow appearance on digital overlay micrographs compared with the single-positive (CD68, green fluorescence) tissue-resident macrophages. Fig. 6*B* demonstrates graphically that A-SAA significantly increased U937 monocyte migration into RA ST ($p < 0.05$).

To determine whether A-SAA directly induces angiogenesis and cell proliferation in vivo, synovial graft cryostat sections were immunostained for anti-VWFVIII and Ki67. A-SAA induced a significant increase in mean blood vessel number/hpf in vivo in synovial graft cryostat sections (Fig. 7*A*, *right panel*) compared with PBS control (Fig. 7*A*, *left panel*). The quantification of A-SAA–induced angiogenesis is illustrated in Fig. 7*B* ($p < 0.05$). A-SAA also induced a significant increase in cell proliferation demonstrated by increased nuclear expression of Ki67 (Fig. 7*C*, *right panel*) compared with PBS control (Fig. 7*C*, *left panel*) ($p < 0.05$). Ki67 was expressed predominantly in the sublining and the vascular endothelium. Quantification of A-SAA–induced proliferation is illustrated in Fig. 7*D*.

Discussion

A-SAA, a rapid response acute-phase protein circulates at very high levels in RA (23) and has been reported in cardiovascular disease (24) and diabetes (25). In chronic inflammation, it may induce amyloidosis and organ failure (26). Furthermore, A-SAA plays a central role in lipid metabolism, and, in the event of acute inflammation, it associates with HDL, displacing Apo-AI and resulting in increased HDL metabolism, reflecting an increased atherogenic potential. The findings of this study considerably extend those of our previous work showing an important pathological role for A-SAA that support the hypothesis that it is a key regulator of proinflammatory events in RA. We demonstrated local

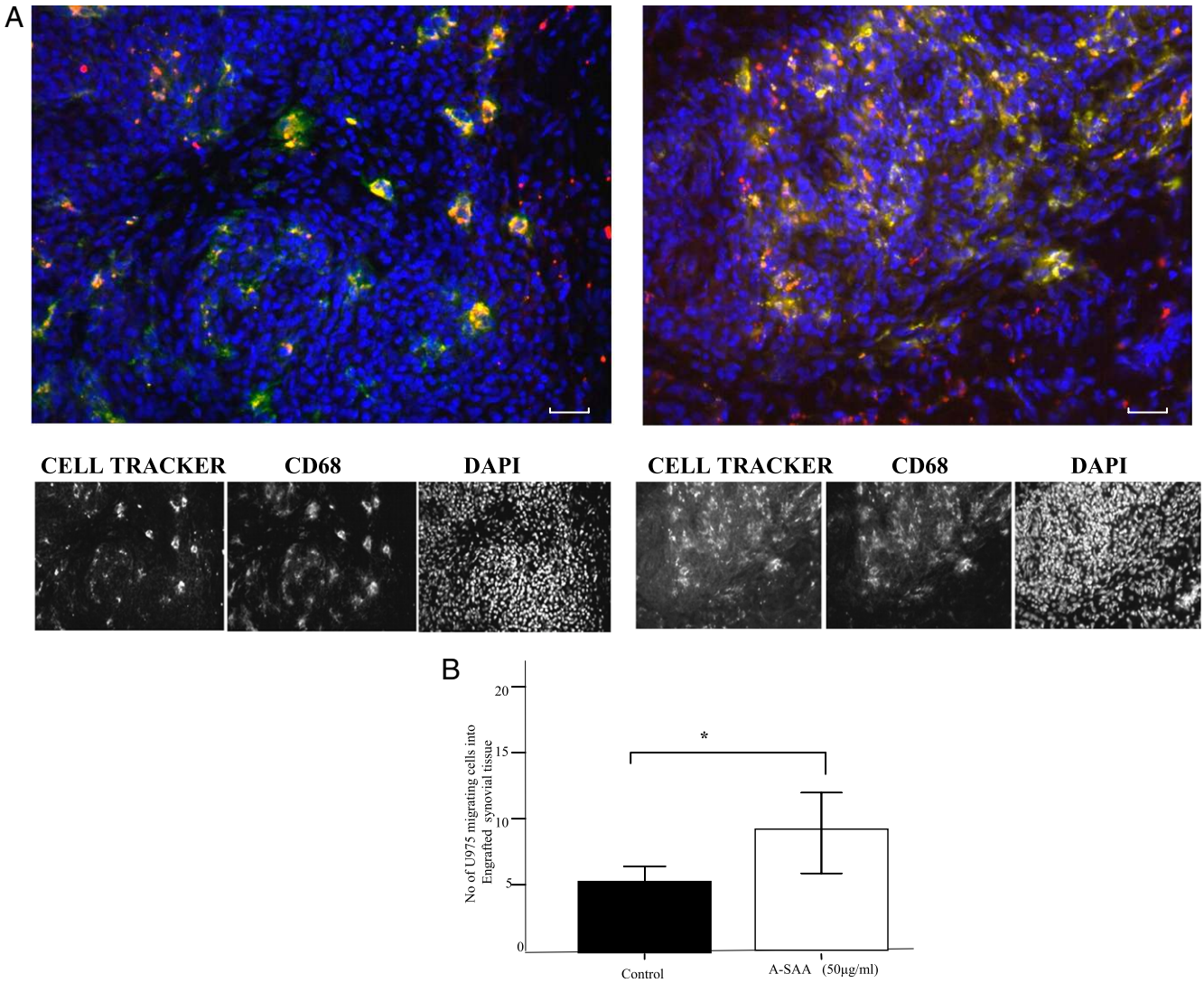

FIGURE 6. A-SAA induces monocyte migration in vivo in a human RA synovial/SCID mouse chimera model. RA ST obtained at arthroscopy was engrafted into SCID mice. At day 14 postengraftment, implants were injected with PBS, A-SAA (50 μg/ml), or TNF-α (10 ng/ml). Following intragraft injection of compounds, animals received an i.v. injection of U937 cells labeled with CellTracker Orange fluorescent probe (red fluorescence). Grafts were harvested, and cryosections were stained for the monocytic marker CD68 and counterstained with the fluorescent nuclear stain DAPI. *A*, Representative images demonstrating minimal monocytic cell staining (double-labeled yellow/yellow-green) in PBS control (*left panel*) compared with A-SAA stimulation (*right panel*). Scale bar, 50 μm; original magnification ×20. *B*, Quantification of monocytic infiltration into synovial grafts shows significant induction by A-SAA compared with control. Values are expressed as the mean ± SEM ($n = 8$). $*p < 0.05$; compared with control.

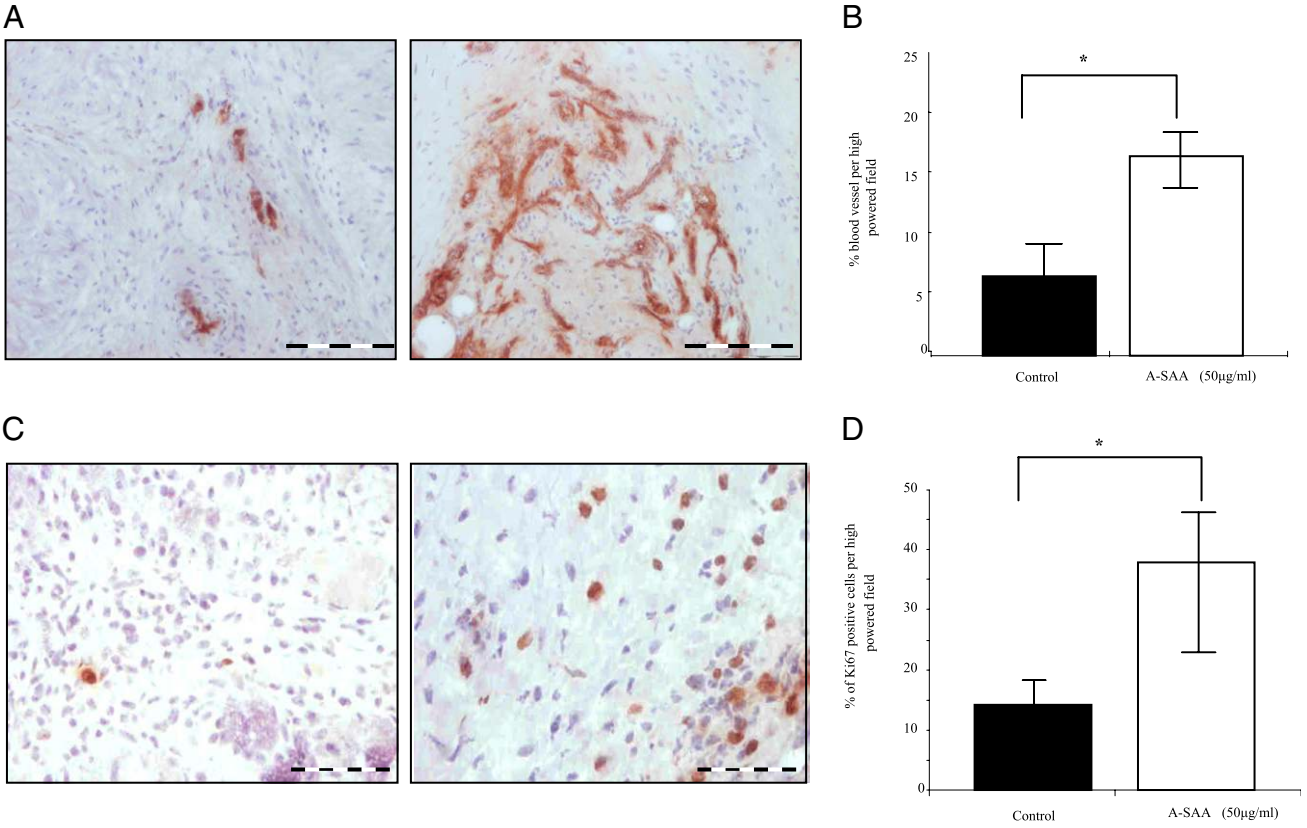

FIGURE 7. A-SAA induces angiogenesis and synovial proliferation in vivo in a human RA synovial/SCID mouse chimera model. *A*, Representative images demonstrating anti-VWFVIII expression on synovial grafts following stimulation with A-SAA (*right panel*) compared with PBS (*left panel*). Scale bar, 200 μm; original magnification ×10. *B*, Bar graphs showing vessel quantification. A-SAA significantly increases blood vessel number compared with PBS control. *C*, Representative images demonstrating immunohistochemistry for the proliferation marker Ki67 synovial grafts following A-SAA stimulation (*right panel*) compared with PBS control (*left panel*). Scale bar, 20 μm; original magnification ×20. *D*, Bar graphs demonstrating quantification of cell proliferation following stimulation with A-SAA compared with PBS control. Values are expressed as the mean ± SEM ($n = 8$). $*p < 0.05$, compared with control.

expression of A-SAA in RA ST explants and SF, which were significantly higher than PsA, OA, and healthy controls. We showed that A-SAA induces chemokine expression in HMECs, RASFCs, and RA ST explants. No significant induction of IL-8 or MCP-1 was shown in PsA synovial explants, suggesting differential A-SAA mechanisms in RA versus PsA. We demonstrated that inhibition of two A-SAA receptors, SR-B1 and FRPL-1, inhibited MCP-1 and IL-8 production, suggesting that they mediate the effects of endogenously produced A-SAA. We also demonstrated that A-SAA induces neutrophil transmigration, monocyte migration, PBMC adhesion, and HMEC invasion, processes that are blocked by the inhibition of IL-8 and MCP-1. In addition, we showed that A-SAA–induced chemokine expression is mediated through NF-κB signaling. Finally, using an in vivo model, we demonstrated that A-SAA directly induces monocyte lineage migration, EC proliferation, and angiogenesis in RA ST engrafted into SCID mice, an effect similar to that seen with TNF-α. These results suggest a direct pathogenic role for A-SAA in driving the proinflammatory response in RA.

A-SAA gene expression and spontaneous release of A-SAA from RA synovial explant cultures ex vivo, a model that maintains tissue architecture of inflamed joint tissue (27), suggests that high circulating levels of A-SAA in RA serum result, at least in part, from a high local production in the joint. This is consistent with previous reports showing that circulating and locally produced A-SAA is highly elevated during various pathological conditions. Although hepatocytes are the major source of A-SAA (28), extrahepatic production was demonstrated in brain, lung, skin, breast, thyroid, and the gastrointestinal tract (29). Previous work from us and other groups (22, 13) showed colocalized expression of A-SAA and its receptors in the vascular endothelium and lining layer of patients with RA, suggesting that A-SAA may induce cellular phenotypic changes locally in the joint. Furthermore, we demonstrated that A-SAA induces IL-8 and MCP-1 expression in HMECs, RASFCs, and RA ST cultures. The functional significance of A-SAA was further demonstrated by showing that A-SAA–induced leukocyte cell migration and PBMC adhesion were inhibited by anti–IL-8 and anti–MCP-1. This further supports a role for A-SAA that had been suggested by previous studies, showing synovial distribution corresponds closely with regions of leukocyte recruitment and angiogenesis. In addition, we and other investigators showed that A-SAA induces adhesion molecules and is chemotactic for T cells, monocytes, and HUVECs (30, 14).

Chemokines are important mediators in inflammation; in the context of RA, they play a critical role in inducing the influx of neutrophils, monocytes, and lymphocytes into the synovium at an early stage of disease, resulting in an invasive pannus and joint swelling. IL-8 and MCP-1 are highly expressed in RA ST and SF, with macrophages being a dominant source (31–33). IL-8 is mainly involved in leukocyte chemotaxis, whereas MCP-1 can attract monocytes, T cells, and NK cells. In addition to their chemoattractant effects, the induction of IL-8 and MCP-1 by A-SAA in synovial cells may have other direct biological effects within the joint. In RASFCs and chondrocytes, MCP-1 can induce cell proliferation, cytokines, and MMPs that contribute to cartilage

destruction (34, 35). Furthermore, the induction of IL-8 was demonstrated in primary articular chondrocytes and cartilage explants, creating a chemoattractant gradient between the cartilage and neutrophils and possibly inducing localized erosion (36). Consistent with this concept, in this study we also demonstrated that activation of HMECs with A-SAA results in several key processes involved in inflammation, such as invasion, PBMC adhesion, and transendothelial cell migration, processes mediated by IL-8 and MCP-1. In addition to its chemoattractant functions, we demonstrated that MCP-1 mediates A-SAA–induced adhesion. This is a novel finding; although the mechanism involved is unclear, previous studies demonstrated that MCP-1 can directly induce ICAM expression. This would support our previous work in which we demonstrated that A-SAA induced ICAM and VCAM expression in HMECs and RASFCs (37, 14) and suggests that A-SAA–induced adhesion may be a direct or indirect effect mediated by MCP-1. Therefore, A-SAA–induced pathologic changes in synovial cells and HMECs facilitate EC activation and leukocyte/monocyte adhesion, migration, and invasion, processes central to the destruction of adjacent cartilage and bone (27, 38–40).

In vitro models, and even in vivo mouse models, often do not fully represent the pathogenic mechanisms of the human immune system. In a recent *Nature* review, Lowes et al. (41) suggested that immunodeficient mice with human tissue xenotransplants provide an ideal model for the dissection of molecular pathways and testing of therapeutic targets. In this study, we examined the in vivo potential of A-SAA using a human-SCID mouse xenograft model. SCID mice were transplanted with human RA synovium that was injected with A-SAA, whereas U937 monocyte cells [a promyelomonocytic cell line that we previously showed to act as good surrogate for human monocytes in this model (20)] were introduced into the mouse circulation. A-SAA significantly induced the migration of U937 cells into RA synovial grafts. Furthermore, we demonstrated that A-SAA significantly increased angiogenesis and cell proliferation in the synovial graft. Monocyte migration did not correlate with vascularity, indicating that A-SAA has a direct, but distinct, action on monocyte chemotaxis and angiogenesis. This is the first report to demonstrate a direct effect of A-SAA on cell migration, proliferation, and angiogenesis in human RA joint tissue in an in vivo model. We and other investigators described that A-SAA directly increases angiogenesis in vitro (14, 42) and via its receptor FPRL-1 can directly stimulate the formation of capillary tubes in a mouse Matrigel assay in vivo (43). Intriguingly, these data also raise the possibility of a link, via disturbed lipid metabolism, among the acute-phase response, chronic systemic inflammation, and cardiovascular risk.

Studies showed that A-SAA via FPRL-1 could regulate several proinflammatory processes (22, 37, 44, 45). Furthermore, studies showed an alternative receptor-signaling pathway for A-SAA: SR-B1, which acts as a receptor for Apo-AI, a constituent of HDL (16). We recently demonstrated the strong expression of SR-B1 on RA synovial vascular endothelium and lining layer and demonstrated that A-SAA proinflammatory effects are mediated, in part, by SR-B1 in HMECs (46). The histological distribution of FRPL-1 and SR-B1 in the inflamed synovium corresponds closely with A-SAA and Apo-AI in RA, suggesting possible receptor–ligand interactions between these apoproteins and their receptor in vivo (7, 47). Specifically, our previous studies demonstrated that A-SAA is expressed in ST synoviocytes and macrophages in the lining layer, in sublining macrophages and ECs (7, 13). In this study, we also showed high expression of A-SAA in RA synoviocytes and neutrophils. Although SAA and its receptors are expressed in RA and PsA patients, the more specific responses in RA patients compared with PsA patients suggest differential pathological mechanisms. Although the precise mechanisms are unclear, work from several groups demonstrated a significant increase in lining layer thickness (macrophages and SFCs) and sublining layer expression of macrophages in RA patients compared with PsA patients (48, 49) Furthermore, a recent study by Vandooren et al. (50) showed that the local inflammatory milieu is clearly different in PsA patients compared with RA patients. They demonstrated that, despite a similar degree of inflammation between the two groups, there is an absence of a classically activated macrophage cytokine signature, such as TNF-α and IL-1β in PsA. Because A-SAA is localized to macrophages and the lining layer, and these cells are significantly more common in RA and produce much higher levels of M1 proinflammatory mediators, it supports the concept of differential inflammatory mechanisms in RA, which may include A-SAA–induced effects.

In this study, we demonstrated inhibition of A-SAA–induced IL-8 and MCP-1 production in RA synovial explant cultures using NAC (a known inhibitor of NF-κB). We showed upregulation of NF-κB expression in RA explants and HMECs in response to A-SAA, which confirms our earlier observation that A-SAA–induced IκBα degradation and nuclear translocation of the p65 subunit in RASFCs and HMECs mediates ICAM-1, VCAM-1, and MMP-1 expression (14). Additionally, studies by Jijon et al. (51) showed that A-SAA induced proinflammatory responses in neutrophils, fibroblast-like synoviocytes, and epithelial cells via NF-κB. This supports recent data by Cheng et al. (17), who reported that TLR2 is a functional receptor for A-SAA where NF-κB luciferase activity is increased in mouse macrophages. TLRs have been implicated to play an important role in RA disease pathogenesis. Previous studies localized TLR2 expression to the RA synovial lining layer and on synovial macrophages (52), which is consistent with the localized expression of A-SAA, further supporting a possible role for TLR2 in the A-SAA–mediated response in RA

In conclusion, A-SAA has traditionally been viewed as an acute-phase reactant and potential biomarker in inflammation, similar to C-reactive protein. In this study, we described critical proinflammatory functions in human cells and tissues to suggest that A-SAA is a functionally relevant proinflammatory molecule. We have shown its relevance to vascular endothelium and RA synovial cells in vitro and in vivo, whereas other investigators recently demonstrated that SAA is a functional ligand, via direct interaction with TLR2, in response to infection. These data in RA cells/tissues and human endothelium provide strong evidence for a common molecular link between A-SAA and the pathogenesis of vascular and joint inflammation.

Disclosures

The authors have no financial conflicts of interest.

References

1. Linke, R. P., J. D. Sipe, P. S. Pollock, T. F. Ignaczak, and G. G. Glenner. 1975. Isolation of a low-molecular-weight serum component antigenically related to an amyloid fibril protein of unknown origin. *Proc. Natl. Acad. Sci. USA* 72: 1473–1476.
2. Steel, D. M., J. T. Rogers, M. C. DeBeer, F. C. DeBeer, and A. S. Whitehead. 1993. Biosynthesis of human acute-phase serum amyloid A protein (A-SAA) in vitro: the roles of mRNA accumulation, poly(A) tail shortening and translational efficiency. *Biochem. J.* 291: 701–707.
3. Husby, G., A. Husebekk, B. Skogen, K. Sletten, G. Marhaug, J. Magnus, and V. Syversen. 1988. Serum amyloid A (SAA)—the precursor of protein AA in secondary amyloidosis. *Adv. Exp. Med. Biol.* 243: 185–192.
4. Artl, A., G. Marsche, S. Lestavel, W. Sattler, and E. Malle. 2000. Role of serum amyloid A during metabolism of acute-phase HDL by macrophages. *Arterioscler. Thromb. Vasc. Biol.* 20: 763–772.
5. Salazar, A., J. Maña, C. Fiol, I. Hurtado, J. M. Argimon, R. Pujol, and X. Pinto. 2000. Influence of serum amyloid A on the decrease of high density lipoprotein-cholesterol in active sarcoidosis. *Atherosclerosis* 152: 497–502.

6. O'Hara, R., E. P. Murphy, A. S. Whitehead, O. FitzGerald, and B. Bresnihan. 2000. Acute-phase serum amyloid A production by rheumatoid arthritis synovial tissue. *Arthritis Res.* 2: 142–144.
7. Vreugdenhil, A. C., M. A. Dentener, A. M. Snoek, J. W. Greve, and W. A. Buurman. 1999. Lipopolysaccharide binding protein and serum amyloid A secretion by human intestinal epithelial cells during the acute phase response. *J. Immunol.* 163: 2792–2798.
8. Meek, R. L., S. Urieli-Shoval, and E. P. Benditt. 1994. Expression of apolipoprotein serum amyloid A mRNA in human atherosclerotic lesions and cultured vascular cells: implications for serum amyloid A function. *Proc. Natl. Acad. Sci. USA* 91: 3186–3190.
9. Libby, P. 2002. Inflammation in atherosclerosis. *Nature* 420: 868–874.
10. Sattar, N., D. W. McCarey, H. Capell, and I. B. McInnes. 2003. Explaining how "high-grade" systemic inflammation accelerates vascular risk in rheumatoid arthritis. *Circulation* 108: 2957–2963.
11. Koch, A. E. 1998. Review: angiogenesis: implications for rheumatoid arthritis. *Arthritis Rheum.* 41: 951–962.
12. Mullan, R. H., B. Bresnihan, L. Golden-Mason, T. Markham, R. O'Hara, O. FitzGerald, D. J. Veale, and U. Fearon. 2006. Acute-phase serum amyloid A stimulation of angiogenesis, leukocyte recruitment, and matrix degradation in rheumatoid arthritis through an NF-kappaB-dependent signal transduction pathway. *Arthritis Rheum.* 54: 105–114.
13. O'Hara, R., E. P. Murphy, A. S. Whitehead, O. FitzGerald, and B. Bresnihan. 2004. Local expression of the serum amyloid A and formyl peptide receptor-like 1 genes in synovial tissue is associated with matrix metalloproteinase production in patients with inflammatory arthritis. *Arthritis Rheum.* 50: 1788–1799.
14. Hershkoviz, R., L. Preciado-Patt, O. Lider, M. Fridkin, J. Dastych, D. D. Metcalfe, and Y. A. Mekori. 1997. Extracellular matrix-anchored serum amyloid A preferentially induces mast cell adhesion. *Am. J. Physiol.* 273: C179–C187.
15. Preciado-Patt, L., R. Hershkoviz, M. Fridkin, and O. Lider. 1996. Serum amyloid A binds specific extracellular matrix glycoproteins and induces the adhesion of resting CD4+ T cells. *J. Immunol.* 156: 1189–1195.
16. Baranova, I. N., T. G. Vishnyakova, A. V. Bocharov, R. Kurlander, Z. Chen, M. L. Kimelman, A. T. Remaley, G. Csako, F. Thomas, T. L. Eggerman, and A. P. Patterson. 2005. Serum amyloid A binding to CLA-1 (CD36 and LIMPII analogous-1) mediates serum amyloid A protein-induced activation of ERK1/2 and p38 mitogen-activated protein kinases. *J. Biol. Chem.* 280: 8031–8040.
17. Cheng, N., R. He, J. Tian, P. P. Ye, and R. D. Ye. 2008. Cutting edge: TLR2 is a functional receptor for acute-phase serum amyloid A. *J. Immunol.* 181: 22–26.
18. Youssef, P. P., M. Kraan, F. Breedveld, B. Bresnihan, N. Cassidy, G. Cunnane, P. Emery, O. Fitzgerald, D. Kane, S. Lindblad, et al. 1998. Quantitative microscopic analysis of inflammation in rheumatoid arthritis synovial membrane samples selected at arthroscopy compared with samples obtained blindly by needle biopsy. *Arthritis Rheum.* 41: 663–669.
19. Wahid, S., M. C. Blades, D. De Lord, I. Brown, G. Blake, G. Yanni, D. O. Haskard, G. S. Panayi, and C. Pitzalis. 2000. Tumour necrosis factor-alpha (TNF-alpha) enhances lymphocyte migration into rheumatoid synovial tissue transplanted into severe combined immunodeficient (SCID) mice. *Clin. Exp. Immunol.* 122: 133–142.
20. Blades, M. C., F. Ingegnoli, S. K. Wheller, A. Manzo, S. Wahid, G. S. Panayi, M. Perretti, and C. Pitzalis. 2002. Stromal cell-derived factor 1 (CXCL12) induces monocyte migration into human synovium transplanted onto SCID Mice. *Arthritis Rheum.* 46: 824–836.
21. Rooney, T., P. Roux-Lombard, D. J. Veale, O. FitzGerald, J. M. Dayer, and B. Bresnihan. 2010. Synovial tissue and serum biomarkers of disease activity, therapeutic response and radiographic progression: analysis of a proof-of-concept randomized clinical trial of cytokine blockade. *Ann. Rheum. Dis.* 69: 706–714.
22. He, R., H. Sang, and R. D. Ye. 2003. Serum amyloid A induces IL-8 secretion through a G protein-coupled receptor, FPRL1/LXA4R. *Blood* 101: 1572–1581.
23. Cunnane, G., S. Grehan, S. Geoghegan, C. McCormack, D. Shields, A. S. Whitehead, B. Bresnihan, and O. Fitzgerald. 2000. Serum amyloid A in the assessment of early inflammatory arthritis. *J. Rheumatol.* 27: 58–63.
24. Kosuge, M., T. Ebina, T. Ishikawa, K. Hibi, K. Tsukahara, J. Okuda, N. Iwahashi, H. Ozaki, H. Yano, I. Kusama, et al. 2007. Serum amyloid A is a better predictor of clinical outcomes than C-reactive protein in non-ST-segment elevation acute coronary syndromes. *Circ. J.* 71: 186–190.
25. Hatanaka, E., P. T. Monteagudo, M. S. M. Marrocos, and A. Campa. 2007. Interaction between serum amyloid A and leukocytes - a possible role in the progression of vascular complications in diabetes. *Immunol. Lett.* 108: 160–166.
26. Piirainen, H. I., A. T. Helve, T. Törnroth, and T. E. Pettersson. 1989. Amyloidosis in mixed connective tissue disease. *Scand. J. Rheumatol.* 18: 165–168.
27. Fearon, U., R. Mullan, T. Markham, M. Connolly, S. Sullivan, A. R. Poole, O. FitzGerald, B. Bresnihan, and D. J. Veale. 2006. Oncostatin M induces angiogenesis and cartilage degradation in rheumatoid arthritis synovial tissue and human cartilage cocultures. *Arthritis Rheum.* 54: 3152–3162.
28. Betts, J. C., M. R. Edbrooke, R. V. Thakker, and P. Woo. 1991. The human acute-phase serum amyloid A gene family: structure, evolution and expression in hepatoma cells. *Scand. J. Immunol.* 34: 471–482.
29. Urieli-Shoval, S., R. P. Linke, and Y. Matzner. 2000. Expression and function of serum amyloid A, a major acute-phase protein, in normal and disease states. *Curr. Opin. Hematol.* 7: 64–69.
30. Furlaneto, C. J., and A. Campa. 2000. A novel function of serum amyloid A: a potent stimulus for the release of tumor necrosis factor-alpha, interleukin-1beta, and interleukin-8 by human blood neutrophil. *Biochem. Biophys. Res. Commun.* 268: 405–408.
31. Koch, A. E., S. L. Kunkel, J. C. Burrows, H. L. Evanoff, G. K. Haines, R. M. Pope, and R. M. Strieter. 1991. Synovial tissue macrophage as a source of the chemotactic cytokine IL-8. *J. Immunol.* 147: 2187–2195.
32. Harigai, M., M. Hara, T. Yoshimura, E. J. Leonard, K. Inoue, and S. Kashiwazaki. 1993. Monocyte chemoattractant protein-1 (MCP-1) in inflammatory joint diseases and its involvement in the cytokine network of rheumatoid synovium. *Clin. Immunol. Immunopathol.* 69: 83–91.
33. Szekanecz, Z., and A. E. Koch. 2001. Chemokines and angiogenesis. *Curr. Opin. Rheumatol.* 13: 202–208.
34. García-Vicuña, R., M. V. Gómez-Gaviro, M. J. Domínguez-Luis, M. K. Pec, I. González-Alvaro, J. M. Alvaro-Gracia, and F. Díaz-González. 2004. CC and CXC chemokine receptors mediate migration, proliferation, and matrix metalloproteinase production by fibroblast-like synoviocytes from rheumatoid arthritis patients. *Arthritis Rheum.* 50: 3866–3877.
35. Borzì, R. M., I. Mazzetti, L. Cattini, M. Uguccioni, M. Baggiolini, and A. Facchini. 2000. Human chondrocytes express functional chemokine receptors and release matrix-degrading enzymes in response to C-X-C and C-C chemokines. *Arthritis Rheum.* 43: 1734–1741.
36. Recklies, A. D., and E. E. Golds. 1992. Induction of synthesis and release of interleukin-8 from human articular chondrocytes and cartilage explants. *Arthritis Rheum.* 35: 1510–1519.
37. Xu, L., R. Badolato, W. J. Murphy, D. L. Longo, M. Anver, S. Hale, J. J. Oppenheim, and J. M. Wang. 1995. A novel biologic function of serum amyloid A. Induction of T lymphocyte migration and adhesion. *J. Immunol.* 155: 1184–1190.
38. Kimball, E. S., and J. L. Gross. 1991. Angiogenesis in pannus formation. *Agents Actions* 34: 329–331.
39. Cawston, T. E., V. A. Curry, C. A. Summers, I. M. Clark, G. P. Riley, P. F. Life, J. R. Spaull, M. B. Goldring, P. J. Koshy, A. D. Rowan, and W. D. Shingleton. 1998. The role of oncostatin M in animal and human connective tissue collagen turnover and its localization within the rheumatoid joint. *Arthritis Rheum.* 41: 1760–1771.
40. Firestein, G. S. 2003. Evolving concepts of rheumatoid arthritis. *Nature* 423: 356–361.
41. Lowes, M. A., A. M. Bowcock, and J. G. Krueger. 2007. Pathogenesis and therapy of psoriasis. *Nature* 445: 866–873.
42. Lee, D. M., H. P. Kiener, S. K. Agarwal, E. H. Noss, G. F. Watts, O. Chisaka, M. Takeichi, and M. B. Brenner. 2007. Cadherin-11 in synovial lining formation and pathology in arthritis. *Science* 315: 1006–1010.
43. Lee, M. S., S. A. Yoo, C. S. Cho, P. G. Suh, W. U. Kim, and S. H. Ryu. 2006. Serum amyloid A binding to formyl peptide receptor-like 1 induces synovial hyperplasia and angiogenesis. *J. Immunol.* 177: 5585–5594.
44. Migita, K., Y. Kawabe, M. Tominaga, T. Origuchi, T. Aoyagi, and K. Eguchi. 1998. Serum amyloid A protein induces production of matrix metalloproteinases by human synovial fibroblasts. *Lab. Invest.* 78: 535–539.
45. Sodin-Semrl, S., A. Spagnolo, R. Mikus, B. Barbaro, J. Varga, and S. Fiore. 2004. Opposing regulation of interleukin-8 and NF-kappaB responses by lipoxin A4 and serum amyloid A via the common lipoxin A receptor. *Int. J. Immunopathol. Pharmacol.* 17: 145–156.
46. Mullan, R. H., J. McCormick, M. Connolly, B. Bresnihan, D. J. Veale, and U. Fearon. 2010. A role for the high density lipoprotein SR-B1 in synovial inflammation via serum amyloid-A. *Am. J. Pathol.* 176: 1999–2008.
47. Bresnihan, B., M. Gogarty, O. FitzGerald, J. M. Dayer, and D. Burger. 2004. Apolipoprotein A-I infiltration in rheumatoid arthritis synovial tissue: a control mechanism of cytokine production? *Arthritis Res. Ther.* 6: R563–R566.
48. Veale, D., G. Yanni, S. Rogers, L. Barnes, B. Bresnihan, and O. Fitzgerald. 1993. Reduced synovial membrane macrophage numbers, ELAM-1 expression, and lining layer hyperplasia in psoriatic arthritis as compared with rheumatoid arthritis. *Arthritis Rheum.* 36: 893–900.
49. Kruithof, E., D. Baeten, L. De Rycke, B. Vandooren, D. Foell, J. Roth, J. D. Cañete, A. M. Boots, E. M. Veys, and F. De Keyser. 2005. Synovial histopathology of psoriatic arthritis, both oligo- and polyarticular, resembles spondyloarthropathy more than it does rheumatoid arthritis. *Arthritis Res. Ther.* 7: R569–R580.
50. Vandooren, B., T. Noordenbos, C. Ambarus, S. Krausz, T. Cantaert, N. Yeremenko, M. Boumans, R. Lutter, P. P. Tak, and D. Baeten. 2009. Absence of a classically activated macrophage cytokine signature in peripheral spondylarthritis, including psoriatic arthritis. *Arthritis Rheum.* 60: 966–975.
51. Jijon, H. B., K. L. Madsen, J. W. Walker, B. Allard, and C. Jobin. 2005. Serum amyloid A activates NF-kappaB and proinflammatory gene expression in human and murine intestinal epithelial cells. *Eur. J. Immunol.* 35: 718–726.
52. Seibl, R., T. Birchler, S. Loeliger, J. P. Hossle, R. E. Gay, T. Saurenmann, B. A. Michel, R. A. Seger, S. Gay, and R. P. Lauener. 2003. Expression and regulation of Toll-like receptor 2 in rheumatoid arthritis synovium. *Am. J. Pathol.* 162: 1221–1227.